Zhao *et al.*
EURASIP Journal on Advances in Signal Processing (2023) 2023:3
https://doi.org/10.1186/s13634-022-00966-0

EURASIP Journal on Advances in Signal Processing

RESEARCH Open Access

Precoding-based complex field network coding strategy for multi-source UAV cooperative system

Mingfei Zhao, Rui Xue* and Hang Jiang

*Correspondence:
xuerui0216@hotmail.com

College of Information and Communication Engineering, Harbin Engineering University, Harbin, China

Abstract

Relay-based UAV swarm can further expand the surveillance range for more complex missions. Microsatellite swarms provide invulnerability and stability compared to conventional satellites and are selected for multi-UAVs multi-satellites systems. Determining how to recover more valuable information from the multi-source data is of significant importance. Considering that vast amounts of multi-source data from UAV swarm require higher throughput performance of transmission schemes, complex field network coding (CFNC) is selected for UAV cooperative system. However, adverse effects like inter-user interference of fading channels will limit the reliability performance of UAV cooperative system. To improve the reliability performance and recover more accurate valuable information, we propose a precoding-based CFNC strategy for multi-source UAV cooperative system. The proposed transmission scheme processes data through precoding matrix, which is obtained by the transformation of channel state matrix. Compared to conventional CFNC schemes, precoding-based CFNC scheme improves the accuracy of detections. Through theoretical analysis and experimental results, the precoding-based CFNC transmission scheme not only maintains high throughput, but also recover more valuable information and achieves better reliability performance.

Keywords: UAV swarms, Multi-source data, Precoding-based CFNC, Reliability

1 Introduction

With the rapid development of information technology, vast amounts of data are continually generated from various monitoring systems [1]. For unmanned aerial vehicles (UAVs) cooperative systems, novel sensors like aerial imaging radar equipped will generate massive multimedia information [2], which requires higher throughput. Determining how to recover valuable information from the multi-source data is of significant importance for the data return of UAV swarms [3], especially for remote communication equipment. Relay-based cooperation in wireless communication for UAVs has attracted much interest for military and civilian applications [4–6]. Compared to conventional terrestrial infrastructures, the advantages of UAVs include high flexibility, low cost and ease of deployment [7, 8], which makes them preferable when setting up wireless

communications for monitoring missions. UAV swarms are thought to be a prospective application for wireless links due to their multiple application scenes such as forest fire prevention, traffic surveillance, precision agriculture, inspection for protective construction [3], and the delivery of commodities. Investigation and surveillance are important applications for UAVs. However, it becomes increasingly difficult to accomplish intricate missions through a single drone due to limitations of energy resources, investigation efficiency, destroy-resistant ability, the visual field and other factors [9], especially for remote and long-endurance missions. In this situation, the application of several UAVs as a swarm is a development trend for UAV monitoring systems [10].

Multiple drones as a swarm will dramatically improve the working efficiency of a single UAV system to complete a variety of assignments [11]. For remote and long-endurance missions, UAVs transmit data to command and control centers through satellite relays. Conventional large satellites can be applied as relays to transmit data, but they are more likely to be interfered and maintain poor resistance to emergency. Compared to conventional large satellites, microsatellite swarms have potential for broad application due to their flexibility, short construction period and low cost. This makes them an effective solution in special communications, remote sensing and services for emergency response. Since communication devices are increasing rapidly [12], the limitation of equipment resources needs to be considered [13]. Therefore, we adopt UAV swarms and microsatellite swarms as source nodes and relay nodes, respectively, instead of single UAV and conventional large satellites.

The process of data transmission is shown in Fig. 1. The UAV swarm transmits data to the microsatellite swarm and then the microsatellite swarm forwards data to command and control center. Recently, image sensors equipped with each drone have led to increasing information collection and designing a high-efficiency transmission scheme has become an issue of concern. Complex field network coding (CFNC) is considered a solution to data return, which obtains significant throughput performance [14]. CFNC obtains throughput as high as 1/2 symbol per source per channel use (sym/S/CU) [15], which is higher than other network coding schemes, such as physical-layer

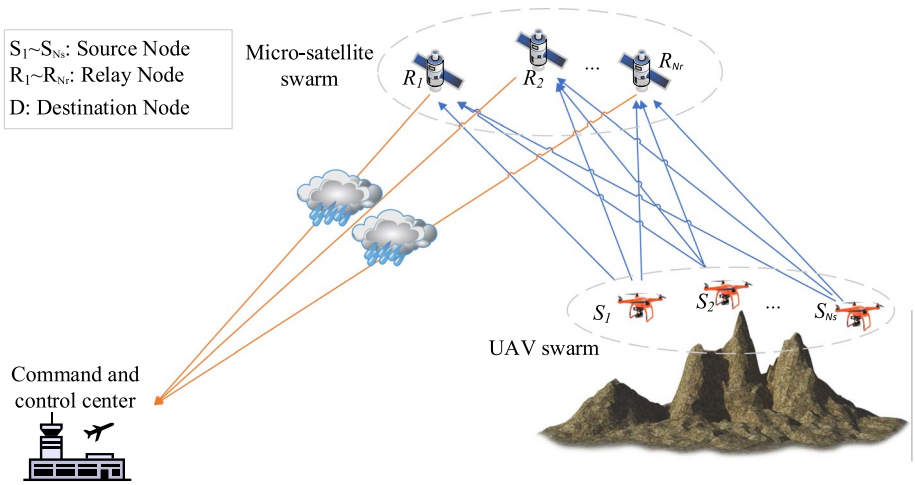

Fig. 1 Regular topology for UAV cooperative network

network coding (PNC), random linear network coding (RLNC) and Galois field network coding (GFNC). CFNC has been adopted in many scenarios for wireless communications for high throughput, such as UAVs [3], wireless backhaul [16], and wireless sensor networks [14]. However, the reliability performance of CFNC is poor while achieving high throughput. As depicted in [15], fading channel leads to adverse effects on CFNC wireless communications, such as multi-user interference and multipath fading, which results in poor performance of symbol error probability (SEP).

The method of signal processing is the key to the quality of transmission [17] when the communication system becomes more and more complicated [18]. For multi-source multi-relay communications, fading channels not only cause energy attenuation, but also intensify multi-user interference. In addition, the influence becomes more obvious as the increasing amounts of data. Reducing the influence of fading channel and improving the reliability performance is crucial to CFNC communications. Therefore, we propose a precoding-based CFNC transmission scheme for UAV swarm system reliability. The transmission scheme requires higher bandwidth for the increasing data and Ka-band is selected for the communications. The most obvious advantage of precoding technology is the reduced complexity at the receiver [19]. The contributions of this paper are shown as follows

1. From the application perspective, we establish a target system that consists of a UAV swarm, a microsatellite swarm and a command and control center. We establish a steady and high bandwidth communication network with destruction resistance for UAV cooperative systems.
2. From the throughput perspective, CFNC exhibits superior performance in throughput, security and bit-level synchronization compared to other NC schemes. Therefore, CFNC is introduced to the UAV cooperative communication system and obviously improves the throughput performance.
3. From the reliability perspective, aiming to improve the quality and reliability performance and attain a compromise algorithm between effectiveness and reliability, an improved precoding-based CFNC transmission scheme is proposed. In addition, the proposed scheme obtains the capacity for channel adaption, which offers reliability performance guarantees for data return.

The rest of this paper is organized as follows: Sect. 2 presents a system model for UAV cooperative communication. Section 3 introduces the link budget for the Ka-band channel. A combination of precoding and CFNC scheme is proposed in Sect. 4. Simulation results and analysis are discussed in Sect. 5. Eventually, we provide the conclusion in Sect. 6.

2 System model for UAV communications

Before NC technology was proposed, relay nodes only stored and forwarded information in the process of data transmission [20]. However, traditional relays require time slots to transmit data, which takes extra time and leads to defects in the real-time performance of the system. The topological structures of the NC and UAV monitoring systems resemble each other if we consider the UAV swarm, microsatellite swarm and the

command and control center as the source, relay and destination, respectively. Therefore, the structure of NC can be applied to UAV cooperative systems.

The transmission principle of conventional schemes, Galois field network coding (GFNC) schemes and CFNC schemes are shown in Fig. 2. Conventional relays transmit information over orthogonal channels to avoid interference, which occupies $N_s(N_r+1)$ time slots. GFNC implements bit level operations, which can improve the performance of throughput to some extent. Different from the conventional transmission scheme, the relay R_1 forwards the Galois field coded symbol to the destination in CU (N_s+1) and the relayR_{N_r} also forwards the Galois field coded symbol to the destination in CU (N_s+N_r) Therefore, the throughput of GFNC system is $1/(N_s+N_r)$ symbol/S/CU. However, the performance of throughput for GFNC is influenced by the number of source nodes and relay nodes. The advantage of throughput is diminished with an increasing number of source and relay nodes.

To break the throughput bottleneck and further reduce transmission time slots, CFNC is applied to the UAV cooperative system in this paper. The information from the source UAV is multiplied by the coding coefficient θ Therefore, the microsatellite relays $R_1, R_2, \ldots, R_{N_r}$ receive the information symbols $\theta_1 x_1, \theta_2 x_2, \ldots, \theta_{N_s} x_{N_s}$ synchronously from $S_1, S_2, \ldots, S_{N_s}$ in CU 1. After maximum likelihood (ML) detections, the estimated symbol $\hat{x}_1, \hat{x}_2, \ldots \hat{x}_N$ are transmitted as $\theta_1\hat{x}_1, \theta_2\hat{x}_2, \ldots \theta_{N_s}\hat{x}_{N_s}$ to the destination in CU 2. Therefore, the number of source nodes and relay nodes will not affect throughput performance of CFNC, which is 1/2 symbol/S/CU. We express the structure of the UAV cooperative system as $N_s - N_r - 1$, which means that the numbers of source nodes, relay nodes and destination node are N_s, N_r and 1, respectively. A remarkable superiority of CFNC transmission scheme is that any problem for a certain drone or microsatellite will not affect the data from other nodes.

The number of channel uses and throughput performance for CFNC, GFNC and conventional scheme are shown in Table 1. Furthermore, CFNC performs symbol level operation, which is easier to meet system synchronization requirements compared to bit level operation of other NC schemes. Compared to other schemes, CFNC occupies the least channel uses and obtains a higher throughput performance. However, the reliability performance of CFNC is poor due to the fading channel and multi-user interference. Therefore, we propose a transmission scheme consist of precoding technology and CFNC. The system diagram of information transmission is depicted in Fig. 3. In the first

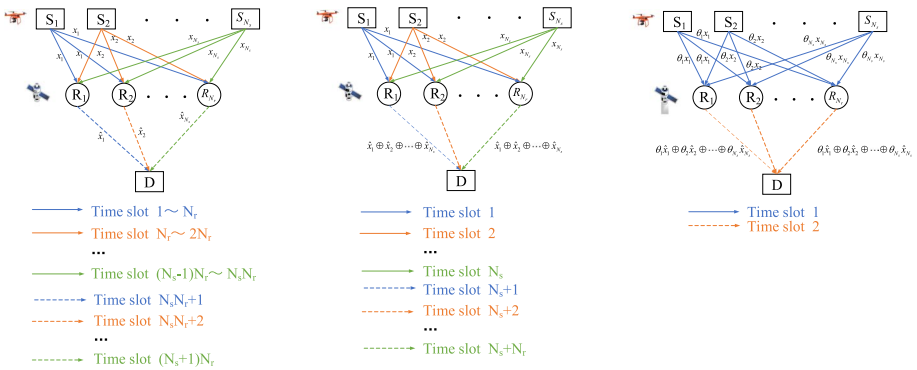

Fig. 2 Transmission principle of NC schemes

Table 1 Real-time performance for different coding schemes

Nerwork coding scheme	Numbers of CUs occupied	Throughput (symbol/source/channel)
Conventional	$N_s(N_r+1)$	$1/N_s(N_r+1)$
GFNC	(N_s+N_r)	$1/(N_s+N_r)$
CFNC	2	1/2

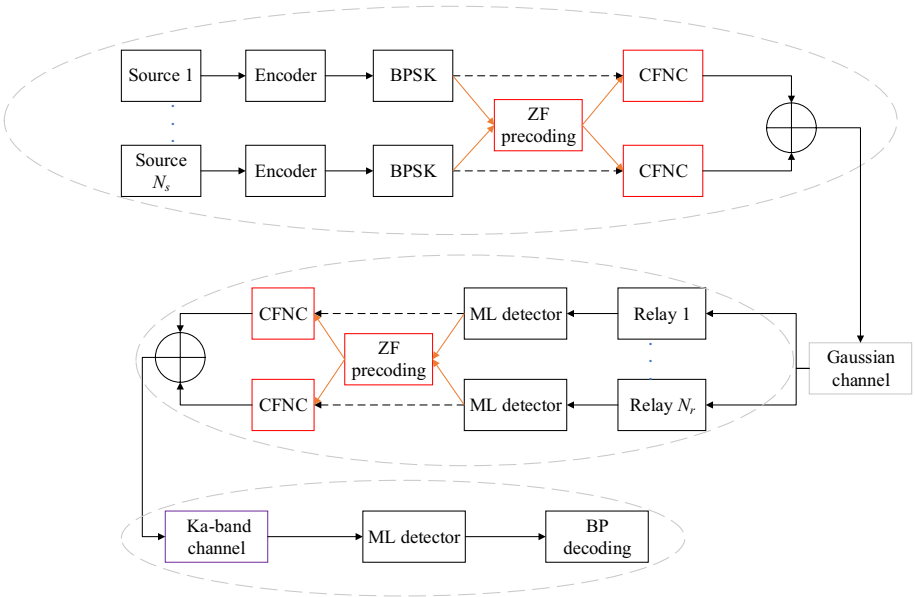

Fig. 3 Information transmission scheme for UAV cooperative system

time slot, the source information is encoded by LDPC code and modulated by binary phase shift keying (BPSK). Then the data are processed by precoding matrix. The matrix of precoding is employed by the channel conditions between UAV swarm and microsatellite swarm. At last, the data are multiplied by the network coding coefficient θ and transmitted to the microsatellite relays. In the second time slot, the information is processed by ML detector. Then each microsatellite relay processes the data by precoding matrix after ML detection. The matrix of precoding is based on the channel condition between microsatellite and command and control center. ML detection in the microsatellite obtains reliability gains. As a result, the precoding technology brings more reliability assurance to the CFNC system. To ensure the applicability of the scheme in the long-distance signal transmission process, link budget for Ka-band channel is introduced in next section.

3 Link budget for Ka-band channel

With the applications of image sensors, the improved efficiency of UAV access to information leads to consistently increasing amounts of data, which requires a higher transmission rate [21]. Conventional frequency bands, such as C, L and Ku band, have been unable to meet the increasing requirements for throughput. Therefore, Ka-band

wireless communication, with high bandwidth, large capacity and strong anti-jamming capabilities, is a solution to this problem and is introduced to the UAV cooperative system in this paper. However, the quality of Ka-band communication has been mainly influenced by attenuations of atmosphere, water vapor, oxygen and rain, especially rain fades [21]. For UAV cooperative systems, signal transmissions require a long distance, which results in severe signal attenuation. In addition, signal transmissions in Ka-band is seriously affected by weather conditions, especially rain attenuations. Therefore, to guarantee the applicability of the proposed scheme in the Ka-band channel, the budgets for the uplink and downlink are discussed in this section.

The purpose of the calculation for the link budget is to evaluate the quality of transmission schemes. Transmission quality of satellite communication links mainly depends on the ratio of carrier power to noise power C/N_0 spectral density at the input side of the system. The C/N_0 in digital satellite communication system determines the symbol error probability (SEP) of the output end of the system, which is a key indicator to measure the transmission quality. The carrier-to-noise ratio C/N_0 can be expressed as C/kT where the carrier power entering the receiving system is C, T represents the equal noise temperature in absolute temperature (K) of the receiving system. k is the Boltzmann constant, which is expressed as $[k] = -228.6$ dBW/(KHz). When the receiver is in the matching state, the noise power can be expressed as $N = kTB$ and kT is power spectral density of the noise. For a digital satellite communication system, the signal-to-noise ratio E_b/N_0 can be calculated as follows

$$C/N_0 = E_b/N_0 + 10 \lg R_b \tag{1}$$

where R_b represents the information transmission rate. Effective isotropic radiated power (EIRP) indicates the capacity of the combination of antenna orientation radiation and the transmitter. EIRP can be indicated as $\text{EIRP} = [P_T + G_T]$, where P_t express the output power of transmitter and G_t expresses the antenna gain of transmitter.

The quality of the transmission scheme is related to factors such as the power of the transmitter, gain of the antenna, various losses in the transmission process and noise performance. Since the Ka-band channel is mainly affected by rain attenuation, we consider the link budget in the following three factors: free space loss, rain attenuation loss and other losses.

Therefore, we can express the basic link equation as follows

$$[C/kT] = [\text{EIRP}] - [L_{\text{FS}}] + [G/T]_R - [k] - [L_0] \tag{2}$$

where L_{FS} is the free space loss, and L_0 indicates other losses and G/T is the quality factor of the receiving system. By employing the analysis above, the uplink equation and downlink equation can be obtained as follows

$$[C/kT]_{\text{UL}} = [\text{EIRP}]_{\text{UAV}} - [L_{\text{FS}}]_{\text{UL}} + [G/T]_{\text{SAT}} - [k] - [L_0] \tag{3}$$

$$[C/kT]_{\text{DL}} = [\text{EIRP}]_{\text{SAT}} - [L_{\text{FS}}]_{\text{DL}} + [G/T]_{\text{EARTH}} - [k] - [L_0] \tag{4}$$

To verify the feasibility of the proposed transmission scheme, we take the base station in Beijing as an example. The height of the low-altitude microsatellite is set to 1175 km, and

Table 2 Parameters for uplink and downlink communication

	Parameters	Values	Units
UPLINK	$[\text{EIRP}]_{\text{UAV}}$	20	dBW
	$[L_{\text{FS}}]_{\text{UL}}$	181.6	dB
	$[G/T]_{\text{SAT}}$	− 5.3	dB/K
	$[k]$	− 228.6	dBW
	R_b	1	Mbit/s
DOWNLINK	$[[\text{EIRP}]_{SAT}$	40.8	dBW
	$[L_{\text{FS}}]_{DL}$	181.8	dB
	$[G/T]_{\text{EARTH}}$	37.7	dB/K
	$[k]$	− 228.6	dBW
	R_b	1	Mbit/s
	$[L_{\text{RA}}]_{\text{DL}}$	13.4	dB

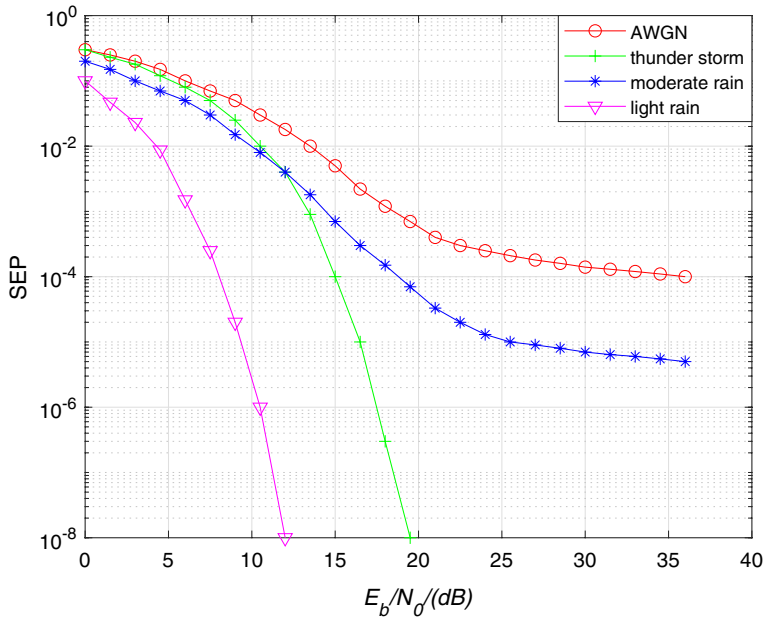

Fig. 4 Information transmission scheme for UAV cooperative system

the flight altitude of the UAV is supposed to be 20 km. The parameters for uplink and downlink communication are shown in Table 2.

In the process of signal transmission, the signal is mainly affected by the atmosphere, including absorption and scattering of signal wave by clouds, rain, and snow. Atmospheric absorption loss mainly includes the absorption loss caused by oxygen and water vapor in the atmosphere to the signal. The influence of different rainfall weather on signal transmission reliability is depicted in Fig. 4. It can be seen that when SEP is in the interval between $[10^{-4}, 10^{-5}]$ the requirement of E_b/N_0 is higher and higher with the increase of rainfall. When the SEP is set at 10^{-5}, the loss of E_b/N_0 is approximately 8–30 dB in different weather conditions. When the E_b/N_0 is 15 dB, the SEP performance is the worst in thunder storms, followed by moderate rain and

light rain. Under the background of light rain, the satisfying the requirement of SEP is 15–17 dB.

In addition to the influence of rain attenuation, the transmission system will also be influenced by other losses in the transmission process, such as polarization mismatch loss, tracking loss, and feeder loss. Compared with the signal attenuation caused by rain, these attenuations are minor, which are set to 5 dB in this paper. As shown in Table 2, the free space loss is calculated as follows

$$[L_{\mathrm{FS}}] = 92.45 + 20\lg d + 20\lg f \tag{5}$$

where d is the distance between the transmitter and the terminal receiver. Other losses such as polarization mismatch loss are set to 5 dB. We suppose that the channel is in the weather of thunder storm, the maximum E_b/N_0 loss caused by rain attenuation is approximately 30 dB. Therefore, we can obtain $[C/kt]_{\mathrm{UL}} = 46.7$ dB and $[C/kt]_{\mathrm{DL}} = 106.9$ dB. Based on (4), E_b/N_0 for the UAV cooperative system has 17 dB gains. Considering the effects of extreme weather, the system has a 17 dB reserve balance for thunder storms, ice pellets and blowing snow, which fully guarantees the operation of the system in poor conditions.

It can be seen that variation in different weather conditions such as rainfall has a significant impact on channel conditions. Villainous weather conditions will worsen channel fading and reduce the system reliability. CFNC has improved the performance of throughput by reducing the time slots of the transmission. However, one of the primary issues in network coding system is the decrease of reliability. In addition, the poor reliability performance is mainly caused by the channel conditions and inter-user interference between UAVs and microsatellites. Therefore, determining how to eliminate the inter-user interference is an effective method to improve the reliability performance. The precoding technology can eliminate the inter-user interference and enhance the channel adaptability of data in CFNC system, which is the key of this paper.

4 Precoding-based CFNC transmission scheme

In conventional UAV-satellite relayed systems, each source UAV uses a different time slot to deliver data, and each satellite relay also uses a different time slot to transmit data. In addition, more time slots are required as the increasing number of source and relay nodes, which leads to poor real-time performance. CFNC, which is applied to wired network system, is introduced to wireless communication system to improve the throughput performance. CFNC can dramatically reduce the number of time slots and enhance the throughput for the UAV cooperative system. The precoding technology can eliminate inter-user interference and enhance the channel adaptability for the CFNC transmission scheme.

For UAV cooperative systems with fixed number of source and relay nodes, the communication links between different types of nodes are the most crucial factor affecting the reliability performance. The regular topology structure of UAV cooperative systems is depicted in Fig. 4. Regular topology structure indicates a direct communication link exists between each different types of nodes. Specifically, each UAV is connected with all microsatellites. In addition, due to the long distance and the obstruction of obstacles, no direct communication links exist between the drone swarm and command and control

center. Similarly, due to the high mobility and the obstruction of obstacles, the source drone cannot maintain direct communication links to microsatellite relays. Therefore, in addition to regular topology structure, we should also consider the impact of irregular topology structure.

As shown in Fig. 4, the topology structure of UAV cooperative system is parallel to the Tanner graph of LDPC code. Therefore, we can express different topology structure by different matrices. Microsatellite relays are not only in a stable position but also in large radiation ranges. The direct communication links between microsatellites and the command and control center are not affected by obstacles, hence we rationally expect that each microsatellite is directly connected with the command and control center. However, the direct communication links between UAV swarm and microsatellite swarm are more likely to be blocked by obstacles due to the characteristics of high mobility and small size of drones. Therefore, we can represent the connection edges between UAV swarm and microsatellite swarm by a matrix **M**.

m_{ij} expresses the element in column j of row i in matrix **M**. The rows and columns of matrix **M** indicate the source drones and relay microsatellites, respectively. When the value of m_{ij} is 1, this means the direct communication link exists between the source UAV S_i and the relay microsatellite R_j. Oppositely, when the value of m_{ij} is 0, this means the direct communication link cannot exist between source UAV S_i and the relay microsatellite R_j. In other words, S_i cannot transmit information to R_j in this case. For conventional regular network coding systems, **M** is expressed as follows

$$\begin{bmatrix} 1 & 1 & \cdots & 1 \\ 1 & 1 & \cdots & 1 \\ \vdots & \vdots & \cdots & \vdots \\ 1 & 1 & \cdots & 1 \end{bmatrix}_{N_r \times N_s} \tag{6}$$

The topology structure in (6) is termed as regular topology structure. Otherwise, we call it irregular topology structure. As mentioned above, we believe that UAVs cannot transmit information to command and control center directly and the direct communication links between microsatellites and command and control center is not affected by obstacles. To make the research more universal, we verify the influence of regular and irregular topology structure on reliability performance, respectively.

As shown in Fig. 3, the source information from source 1 to source N_s are expressed as $[k_1, k_2, \ldots, k_{N_s}]$, we take k_1 the data from source 1, as an example. The information encoded by LDPC can be expressed as follows

$$m_1 = k_1 \cdot \mathbf{G} \tag{7}$$

where **G** is the generated matrix of LDPC code. The generated matrix **G** and the parity check matrix **H** satisfy (8)

$$\mathbf{G} \cdot \mathbf{H}^T = 0 \tag{8}$$

After BPSK modulation, x represents a symbol vector obtained by the constellation mapping of bit sequences. As depicted in Fig. 3, precoding is added to the original CFNC system between the modulation and CFNC. Although CFNC improves the throughput performance of the UAV cooperative system, the reliability is inevitably sacrificed.

Precoding technology computes the precoding matrix according to the channel statement information (CSI), which leads to mutual interference between different subchannels equal to zero. Specifically, the information processing of the precoding scheme is shown in Fig. 5.

In Fig. 5, **F** is the precoding matrix, and parameter β, which is used to control the average power of sending signals, expresses the power control factor. The sending signal s can be represented as follows:

$$s = \beta \mathbf{F} x \tag{9}$$

Considering the channel fading and the effects of additive noise, the receiving signal y can be expressed as follows:

$$y = \mathbf{H}s + n = \beta \mathbf{H}\mathbf{F}x + n \tag{10}$$

where **H** is the channel matrix, and n represents the noise vector at the receiver.

Aiming at zero mutual interference between different users at receivers, the following relationship can be obtained

$$\mathbf{H}\mathbf{F} = \mathbf{I} \tag{11}$$

As depicted in (11), the precoding matrix **F** can be presented as follows:

$$\mathbf{F} = \mathbf{H}^H (\mathbf{H}\mathbf{H}^H)^{-1} \tag{12}$$

In addition, to make the average power of the sending signal lower than the rated sending power P_T of the transmitter, β is introduced. Assuming that the sending data from different drones are independent of each other, the average energy of sending symbol is 1.

$$E\{s^H s\} = \beta^2 E\{x^H \mathbf{F}^H \mathbf{F} x\} = \beta^2 \mathrm{tr}\{\mathbf{F}\mathbf{F}^H\} \tag{13}$$

According to (13) and the power constraint, β can be obtained as follows

$$\beta = \sqrt{P_t / \mathrm{trace}\{\mathbf{F}\mathbf{F}^H\}} \tag{14}$$

Based on (12) and (14), the estimated value of sending symbol $\tilde{x}$ after detection at the receiver can be presented as follows:

$$\tilde{x} = \frac{1}{\beta} y = x + \frac{1}{\beta} n \tag{15}$$

Relay satellites R_1 to R_j process information following the methods above. In the first time slot, each relay receives data from all UAVs. For the UAV cooperative system

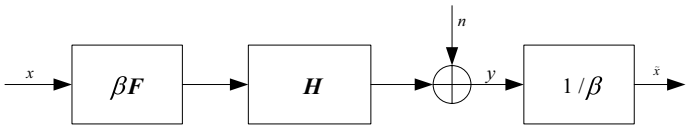

Fig. 5 Information processing of precoding scheme

based on the topology structure $N_s - N_r - 1$, the received symbol at the relay R_j can be expressed as follows

$$\begin{aligned} y_{SR_j}(t) &= h_{S_1R_j}\theta_1 x_1(t) + \cdots h_{S_{N_s}R_j}\theta_{N_s}x_{N_s}(t) + n_{SR_j}(t) \\ &= \theta_S^T \mathbf{H}_{SR_j} x(t) + n_{SR_j}(t) \end{aligned} \tag{16}$$

We can observe that conventional CFNC transmission scheme for UAV cooperative systems is seriously affected by fading channels, which leads to poor SEP performance. On the one hand, the channel coefficient matrix **H** leads to attenuations of signal power; on the other hand, **H** results in multi-user interference, which affects the accurate calculation of Euclidean distance for detections. In addition, the information transmission is affected by two channels due to the employed relays. In summary, the channel coefficient matrix **H** is one of the main factors affecting reliability performance. Therefore, determining how to eliminate the adverse effects of **H** is an effective way to improve reliability performance. For precoding-based CFNC transmission scheme, the symbol processed by precoding matrix received at R_j is expressed as follows

$$\begin{aligned} y_{SR_j}(t) &= h_{S_1R_j}f_{S_1R_j}\theta_1 x_1(t) + \cdots h_{S_{N_s}R_j}f_{S_{N_s}R_j}\theta_{N_s}x_{N_s}(t) + n_{SR_j}(t) \\ &= \theta_S^T \mathbf{H}_{SR_j}\mathbf{F}_{SR_j} x(t) + n_{SR_j}(t) \end{aligned} \tag{17}$$

where $h_{S_1R_j}$ represents the channel coefficient matrix between the source UAV S_1 and the microsatellite relay R_j. Compared to the conventional CFNC system, transmission schemes with precoding technology multiply the information from each source by a precoding matrix to estimate the influence of fading channels. In addition, $\mathbf{H}_{SR_j}$ is given as follows:

$$\mathbf{H}_{SR_j} = \mathrm{diag}\left(h_{S_1R_j}, h_{S_2R_j}, \ldots, h_{S_{S_E}R_j}\right) \tag{18}$$

$\mathbf{H}_{SR_j}$ represents the channel coefficient matrix between the UAV swarm and the microsatellite swarm, which means the current channel state information. $CN\left(0, \sigma_{ij}^2\right)$ demonstrates a Gaussian distribution with mean of 0 and variance of σ_{ij}^2. Therefore, the parameter n_{ij} and σ_{ij}^2. Therefore, the parameter n_{ij} and h_{ij} can be expressed as follows

$$n_{ij} \sim CN(0, N_0) \tag{19}$$

$$h_{ij} - CN\left(0, \sigma_{ij}^2\right) \tag{20}$$

where $f_{S_1R_j}$ is the precoding matrix between the source UAV S_1 and the microsatellite relay R_j. The precoding matrix $f_{S_1R_j}$ can be expressed as follows

$$f_{S_1R_j} = h_{S_1R_j}^H \left(h_{S_1R_j} h_{S_1R_j}^H\right)^{-1} \tag{21}$$

In addition, $\mathbf{F}_{SR_j}$ represents the precoding matrix between the UAV swarm and the microsatellite swarm. $\mathbf{F}_{SR_j}$ can be expressed as follows

$$\mathbf{F}_{SR_j} = \mathrm{diag}\left(f_{SR_j}, f_{S_2R_j}, \ldots, f_{S_{V_i}R_j}\right) \tag{22}$$

$\gamma_{ij} = \left|h_{ij}\right|^2 \bar{\gamma}$ and $\bar{\gamma}_{ij} = \sigma_{ij}^2 \bar{\gamma}$ denote the instantaneous and average signal-to-noise ratios (SNRs), where $\bar{\gamma} = P_x/N_0$ and P_x denote the average transmission power of source symbol x. The information symbol vector $x(t)$ can be demonstrated as follows

$$x(t) = \left[x_1(t), \ldots x_{N_s}(t)\right]^T \tag{23}$$

where $t = 1$,...N_r and $j = 1$,...N_r.

We define the coding coefficient as θ. Before the first time slot, the information x_i from S_i is multiplied by θ. We select the design of the linear complex field (LCF) for the proposed UAV cooperative scheme. The details for the design are expressed in [22], θ_s^T can be presented as follows

$$\theta_s^T = \left[\theta_1, \theta_2, \ldots, \theta_{N_s}\right] \tag{24}$$

The design of θ_s^T is the key to the CFNC scheme, LCF is also applied in MIMO systems. Using the concept and property of Euler numbers, two respective designs of these generators are provided in [23] : $\sigma_n = e^{i\pi(4n-1)/2N_s}$ if $N_s = 2^k$ and $\sigma_n = e^{i\pi(6n-1)/3N_s}$ if $N_s = 3 \times 2^k$, where n indicates the nth row of the Vandermonde matrix, i.e.:

$$\theta = \begin{bmatrix} 1 & \delta_1 & \cdots & \delta_1^{N_s-1} \\ 1 & \delta_2 & \cdots & \delta_2^{N_x-1} \\ \vdots & \vdots & \cdots & \vdots \\ 1 & \delta_{N_s} & \cdots & \delta_{N_s}^{N_s-1} \end{bmatrix} \tag{25}$$

Different from MIMO systems with multiple antennas, the analysis of network of CFNC is more complicated due to the possibilities of error symbols in relay decoding. To improve the reliability performance of the system, microsatellite relays perform ML detection on the received data from the UAV. After N_r relay CUs, the ML of detection at relay R_j is expressed as follows:

$$\hat{x}_j(t) = \arg\min_{x(t)} \left\| y_{SR_j}(t) - \theta_s^T \mathbf{H}_{SR_j} \mathbf{F}_{SR_j} x(t) \right\| \tag{26}$$

where $\hat{x}_j(t)$ is the estimated symbol vector obtained by ML detection.

After the estimated symbol is obtained, $\hat{x}_j(t)$ is processed by precoding matrix and CFNC. The channel coefficient matrix $\mathbf{H}_{R_jD}$ and the precoding matrix $\mathbf{F}_{R_jD}$ are employed by the channel conditions between the microsatellite swarm and command and control center. In the second time slot, the estimated symbol is multiplied by α, which denotes the link-adaptive scalar, and then transmitted to the command and control center. The coding coefficient θ_R is a matrix designed as follows

$$\theta_R^\top = \left[\theta_1, \theta_2, \ldots, \theta_{N_S \times N_r}\right] \tag{27}$$

where $\theta_i = e^{j\pi(4n-1)(i-1)/2n}$ if $N_s \times N_r = 2^k$ and if $N_s \times N_r = 3 \times 2^k$, $\theta_i = e^{j\pi(6n-1)(i-1)/3n}$. θ_R is transformed by $\theta_s^{'}$. The design of $\theta_{R_j}^T$ is based on the number of

source nodes and relay nodes. The relationship of the input/output (I/O) from the jth relay to the destination in the second time slot is as follows

$$y_{R_jD}(t) = \sqrt{\alpha_j} h_{R_jD} f_{R_jD} \theta_R^T \hat{x}_j + n_{R_jD}, j = 1, \ldots, N_r \tag{28}$$

$$\hat{x}_j = \left[\hat{x}_j^T(1), \ldots, \hat{x}_j^T(N_r)\right]^T \tag{29}$$

Finally, the symbol is obtained by ML detection at the destination after two CU transmissions, the result is shown as follows

$$\hat{x}_D = \arg\min \left\{ \sum_{t=1}^{N_r} \sum_{j=1}^{N_T} \left\| y_{R_jD}(t) - \sqrt{\alpha_j} h_{R_jD} f_{R_jD} \theta_R^T x' \right\|^2 \right\} \tag{30}$$

$$x' = \left[x^T(1), \ldots, x^T(N_r)\right]^T \tag{31}$$

5 Numerical results and analysis

In Sect. 2, the throughput performance of conventional, GFNC and CFNC scheme are discussed, and the reliability performance is tested through Monte Carlo simulations in this section. The simulation in this paper ignores the co-channel interference between different UAVs. In addition, SEP is adopted to measure the reliability performance, and the influence of source node numbers, relay node numbers and precoding are discussed. In addition, we verify the effect of regular and irregular topology structure on reliability performance. We set the uplink channel and downlink channel as Gaussian white noise channels and Ka-band fading channels, respectively. The length of the binary information frame is set to 600 bits and the frame number is set to 10,000. Furthermore, the symbol is constituted by each bit in the same position for a certain frame. We compare the precoding-based CFNC scheme with the existing scheme in [3] and select the same irregular topology structure to demonstrate the reliability advantage of precoding-based scheme.

To guarantee the reliability performance of transmission scheme, CFNC is normally combined with channel coding [3]. Therefore, three different coding schemes [repeat-accumulate (RA) codes, turbo codes, and LDPC codes] are selected to the proposed transmission system to verify the influence of source and relay node numbers. We construct the check matrix of the LDPC code by a QC algorithm with Gaussian elimination. The decoding algorithm is belief propagation (BP) and the iteration number is set to 25. The ML algorithm is selected as a detection algorithm for CFNC. In addition, BPSK modulation is adopted for the coded data. We verify the influence of regular and irregular topology structure on reliability performance by simulations primarily. In order to verify the reliability performance gain compared to conventional CFNC schemes, we select the same topology structure to the topology structure in [3]. The matrix **M** for irregular topology structure is shown in Table 3.

As demonstrated in Figs. 6 and 7, we have discussed the influence of precoding matrix on regular and irregular topology structure. We also verify the effect of the

Table 3 The matrix **M** for irregular topology structure

Structure	**6-8-1**	**6-6-1**
M	$\begin{bmatrix} 1&0&0&0&0&0\\ 1&1&0&0&0&0\\ 1&1&1&0&0&0\\ 1&1&1&1&0&0\\ 0&1&1&1&1&0\\ 0&0&1&1&1&1\\ 0&0&0&1&1&1\\ 0&0&0&1&1&1 \end{bmatrix}$	$\begin{bmatrix} 1&1&0&0&0&0\\ 1&1&1&0&0&0\\ 1&1&1&1&0&0\\ 0&1&1&1&1&0\\ 0&0&1&1&1&1\\ 0&0&0&1&1&1 \end{bmatrix}$
6-4-1	4-6-1	8-6-1
$\begin{bmatrix} 1&1&0&0&0&0\\ 1&1&1&1&0&0\\ 0&0&1&1&1&1\\ 0&0&0&0&1&1 \end{bmatrix}$	$\begin{bmatrix} 1&1&0&0\\ 1&1&1&0\\ 1&1&1&0\\ 0&1&1&1\\ 0&1&1&1\\ 0&0&1&1 \end{bmatrix}$	$\begin{bmatrix} 1&1&1&1&0&0&0&0\\ 1&1&1&1&0&0&0&0\\ 0&1&1&1&1&0&0&0\\ 0&0&1&1&1&1&0&0\\ 0&0&0&1&1&1&1&0\\ 0&0&0&0&1&1&1&1 \end{bmatrix}$

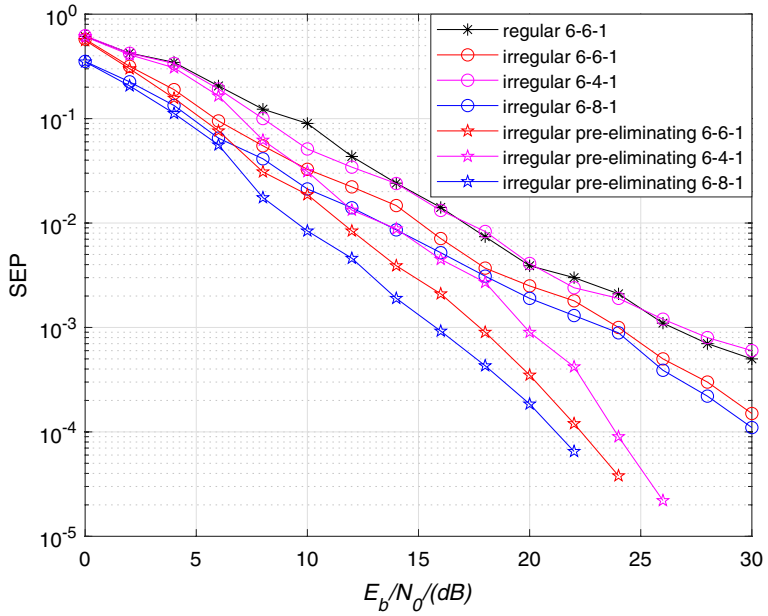

Fig. 6 SEP of precoding algorithms for $6 - N_r - 1$

number of source nodes and relay nodes on SEP. As we see from Fig. 6, the performance of SEP is improved as the increasing number of relay nodes for irregular topology structure when the number of source nodes is fixed. Under the circumstances, the increased number of relay nodes does not always improve SEP performance efficiently, which means the improvement on SEP becomes not obvious when the number of relay nodes is greater than 10. Therefore, we select the transmission scheme with the number of relay nodes less than 10. Through the analysis above, we can conclude that the precoding scheme reduces the SEP performance for irregular topology structure when the number of relay nodes changes.

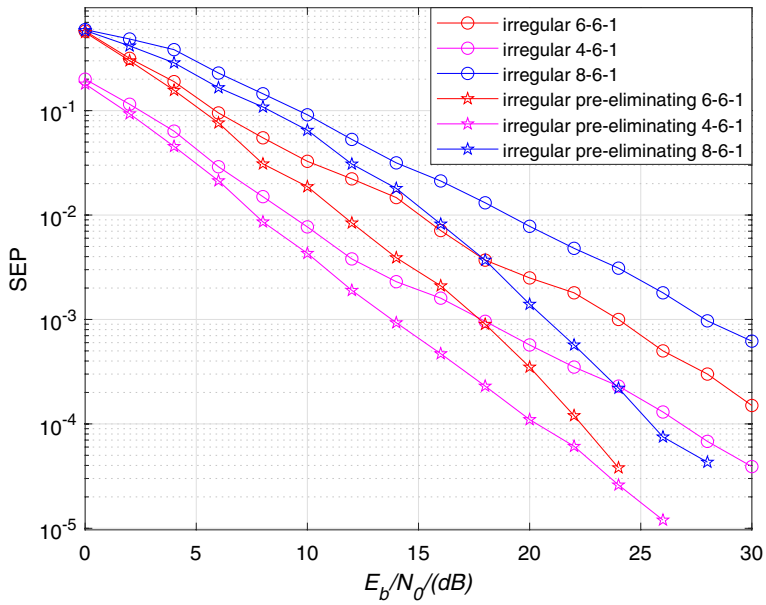

Fig. 7 SEP of precoding algorithms for N_s — 6 — 1irregular CFNC-based topology structure

As we can see from Fig. 7, the performance of SEP becomes worse as the increasing number of source nodes for irregular topology structure when the number of relay nodes is fixed. In addition, the precoding scheme improves the reliability performance of transmission schemes with different numbers of source nodes to some extent. More source nodes lead to more interference, which can be eliminated by precoding matrix. Therefore, precoding scheme works better for CFNC systems with more source nodes. As a result, we can draw a conclusion that precoding matrix improves SEP performance for irregular topology structure with different numbers of source and relay nodes.

We have investigated the reliability performance of the UAV cooperative system in the Ka-band channel with different numbers of source drones and relay microsatellites. And we verify the influence of precoding scheme on different channel coding schemes. Figures 8, 9, and 10 express the SEP performance with different topology structures including [2, 1, 1], [2, 2, 1], [2, 3, 1], [3, 3, 1], [3, 4, 1] for the LDPC codes, Turbo codes, and RA codes, respectively. We conclude that the performance of SEP decreases with an increasing number of microsatellites when the number of drones is fixed. For example, as shown in Fig. 6, when the number of drones is fixed at 2, the structure of [2, 3, 1] earns gains of approximately 3.5 dB compared to the structure of [2, 2, 1] in the region of SEP$= 10^{-4}$. The increasing number of microsatellite relay nodes leads to higher diversity gain origination. Therefore, more relay nodes provide better reliability performance. Similar situations also occur in the other two coding schemes.

The influence on the SEP performance of the source node number can be deduced through the three figures above. Similar simulation results appear for the three coding schemes, and we conclude that the SEP rises with an increasing number of drone nodes when the number of relay microsatellites is fixed. For instance, as depicted in Fig. 10, in case the number of relay nodes is fixed at 3, the structure of [2, 3, 1] earns gains of

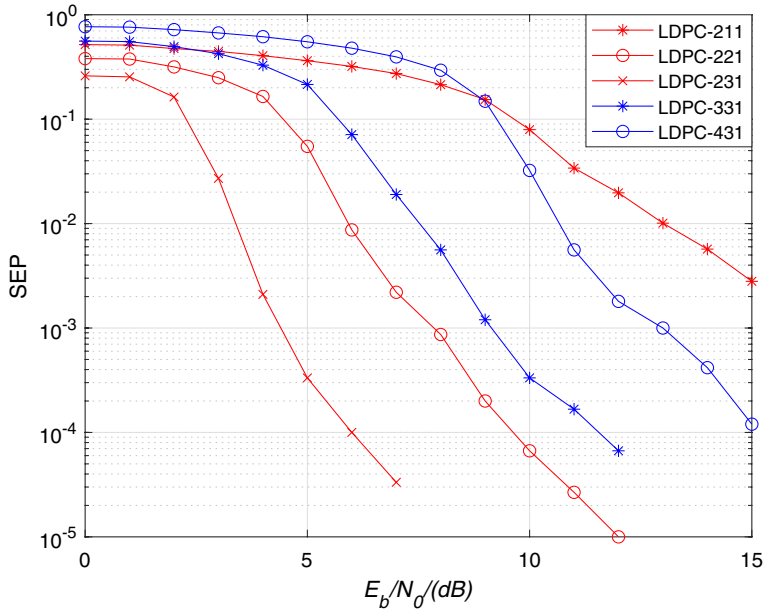

Fig. 8 SEP of LDPC code transmission scheme with different numbers of microsatellites and drones

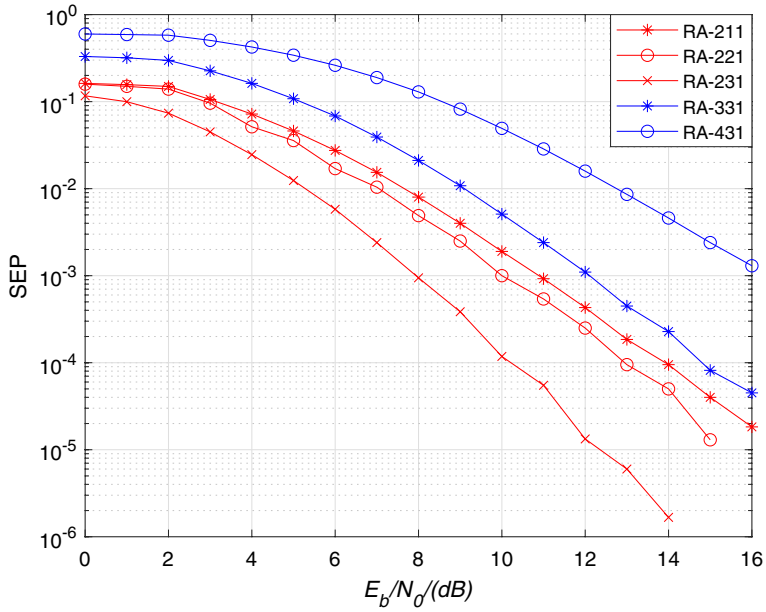

Fig. 9 SEP of RA code transmission scheme with different numbers of microsatellites and drones

over 4 dB compared to the structure of [3, 3, 1] in the region of SEP=10^{-4}. Theoretically, for each relay microsatellite, the more data it receives from different monitoring drones, the worse the SEP performs. Information from different source drones will lead to anti-interference. In addition, the interference caused by data from different drones is enhanced as the amount of information increases, and the relay node will be more likely to make mistakes if it is overloaded, which results in poor SEP performance.

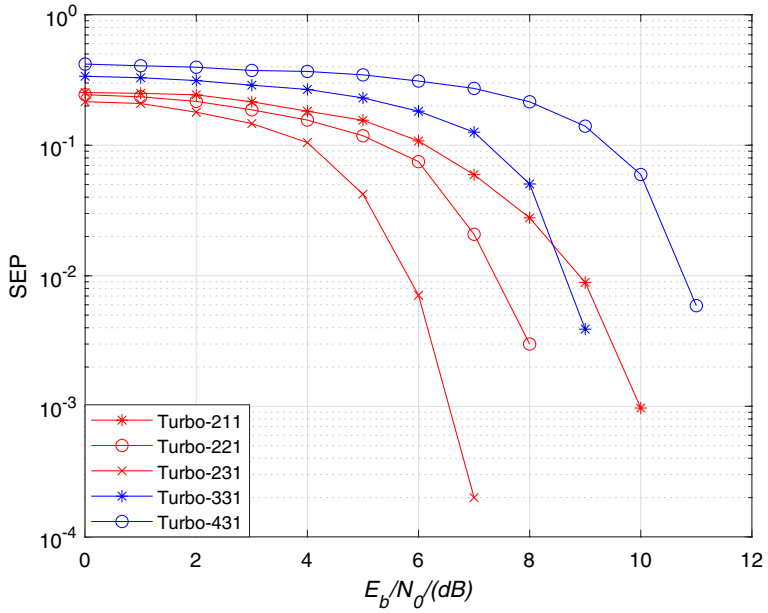

Fig. 10 SEP of turbo code transmission scheme with different numbers of microsatellites and drones

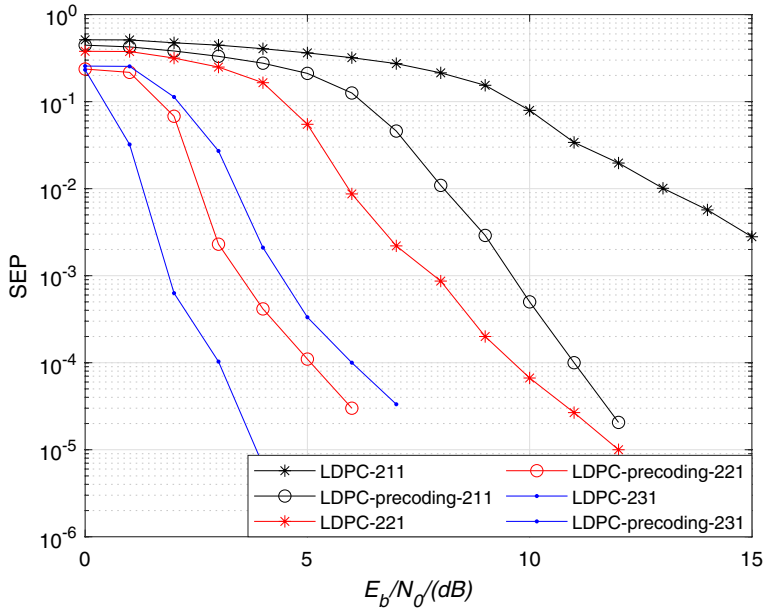

Fig. 11 SEP of precoding algorithms for LDPC codes scheme

For UAV cooperative systems, two primary factors lead to the increasing interference. One is the increasing amount of data due to the image sensors. The other is the increasing number of source nodes and relay nodes. Therefore, to estimate the interference and guarantee SEP performance, the precoding scheme plays a key role in achieving high reliability. Similarly, RA codes, Turbo codes and LDPC codes are selected to verify the SEP improvement for precoding matrix. As shown in Figs. 11, 12 and 13, we take the LDPC code and

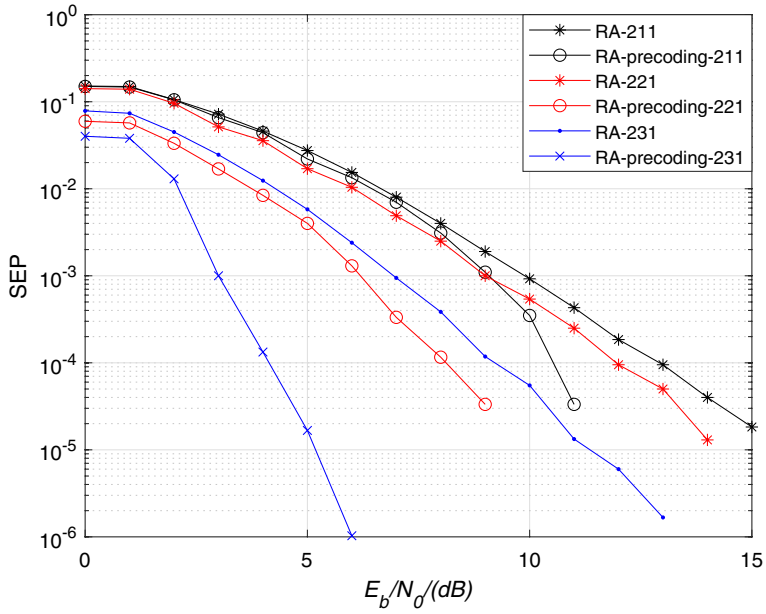

Fig. 12 SEP of precoding algorithms for RA scheme

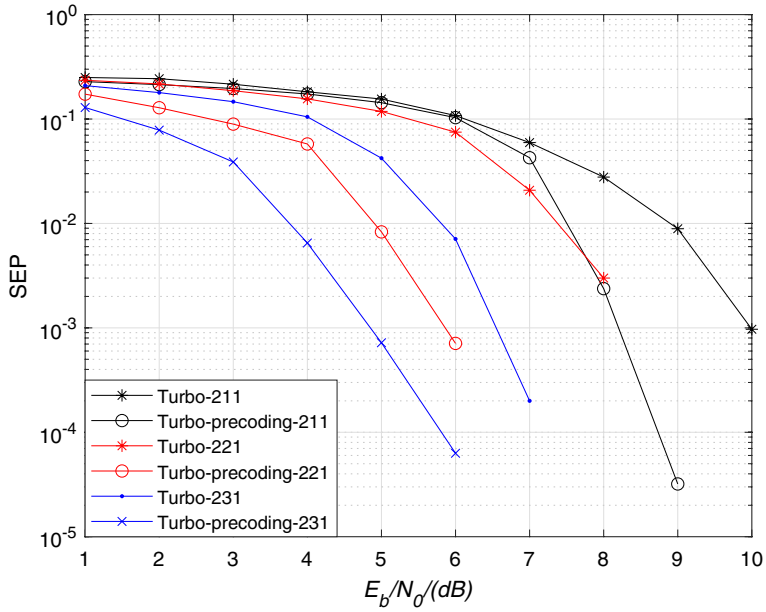

Fig. 13 SEP of precoding algorithms for Turbo scheme

BPSK modulation schemes as examples, and the precoding scheme improves the SEP performance for different topologies. The structure of [2, 3, 1] with the precoding scheme earns approximately 3 dB compared to the original scheme in the region of SEP=10^{-4}. Similarly, the structure of [2, 2, 1] earns 4.5 dB in the region of SEP=10^{-4} and the structure of [2, 1, 1] earns 5 dB when SEP=10^{-2}. RA codes and Turbo codes with precoding matrix also improve the SEP performance to some extent. Therefore, we can draw a conclusion that

precoding improves reliability performance at the sacrifice of the complexity of the UAV cooperative system.

6 Conclusion

To produce effective data return for surveillance UAV swarms, this paper established a system model of UAV swarm microsatellite swarm command and control center communication links in the Ka band. To improve the throughput performance, CFNC was introduced to the system. However, SEP performance of CFNC is poor due to the multi-user interference and multipath fading of fading channels. To improve the quality and reliability performance, we present an improved precoding-based CFNC transmission scheme for UAV swarm reliability performance. In addition, to prove the authenticity of signal transmission, we have carried out the link budget of the UAV communications. Besides the theoretical analysis of the system, we also verify several parameters through simulation experiments, including different topology structures, the number of source nodes and relay nodes, coding schemes and precoding. Simulation results showed that the proposed transmission scheme obtains reliability superior to that of the conventional CFNC scheme for different topology structures, including regular and irregular topology structures, and different channel coding schemes. In addition, the transmission scheme proposed in this paper maintains the 1/2 symbol/source/CU throughput performance. Network communications of UAV swarms and microsatellite swarms are important components of device-to-device communications. The transmission scheme proposed in this paper provides a reliable solution to network communication when maintaining high throughput performance. According to different channel conditions, the transmission scheme offers a compromise between effectiveness and reliability to satisfy different communication requirements in practical applications.

Acknowledgements
Not applicable.

Author contributions
MZ is responsible for conceptualization, methodology and software. RX performed data curation, writing—Original draft preparation. HJ participate in writing, reviewing and editing. All authors read and approved the final manuscript.

Funding
This paper was supported in part by the National Natural Science Foundation of China (No. 61873070), the Heilongjiang Provincial Natural Science Foundation of China (No. LH2020F018), the Fundamental Research Funds for the Central Universities (No. 3072022QBZ0803)

Availability of data and materials
Please contact author for data requests.

Declarations

Ethics approval and consent to participate
Not applicable.

Consent for publication
The picture materials quoted in this article have no copyright requirements, and the source has been indicated.

Competing interests
The authors declare that they have no competing interests.

Received: 21 October 2022 Accepted: 16 December 2022
Published online: 04 January 2023

References

1. Y. Kang, F. Zhang, W. Peng, S. Gao, J. Rao, F. Duarte, C. Ratti, Understanding house price appreciation using multi-source big geo-data and machine learning. Land Use Policy **111**, 104919 (2021)
2. B. Zong, C. Fan, X. Wang, X. Duan, B. Wang, J. Wang, 6g technologies: key drivers, core requirements, system architectures, and enabling technologies. IEEE Veh. Technol. Mag. **14**(3), 18–27 (2019)
3. R. Xue, L. Han, H. Chai, Complex field network coding for multi-source multi-relay single-destination UAV cooperative surveillance networks. Sensors **20**(6), 1542 (2020)
4. G. Wang, B.-S. Lee, J.Y. Ahn, G. Cho, A UAV-aided cluster head election framework and applying such to security-driven cluster head election schemes: a survey. Secur. Commun. Netw. (2018). https://doi.org/10.1155/2018/6475927
5. J. Guo, I. Ahmad, K. Chang, Classification, positioning, and tracking of drones by hmm using acoustic circular microphone array beamforming. EURASIP J. Wirel. Commun. Netw. **2020**(1), 1–19 (2020)
6. P. Ladosz, H. Oh, G. Zheng, W.-H. Chen, Gaussian process based channel prediction for communication-relay UAV in urban environments. IEEE Trans. Aerosp. Electron. Syst. **56**(1), 313–325 (2019)
7. K. Miranda, A. Molinaro, T. Razafindralambo, A survey on rapidly deployable solutions for post-disaster networks. IEEE Commun. Mag. **54**(4), 117–123 (2016)
8. H.N. Qureshi, A. Imran, On the tradeoffs between coverage radius, altitude, and beamwidth for practical UAV deployments. IEEE Trans. Aerosp. Electron. Syst. **55**(6), 2805–2821 (2019)
9. D. He, Y. Qiao, S. Chan, N. Guizani, Flight security and safety of drones in airborne fog computing systems. IEEE Commun. Mag. **56**(5), 66–71 (2018)
10. V. Sharma, R. Kumar, Cooperative frameworks and network models for flying ad hoc networks: a survey. Concur. Comput. Pract. Exp. **29**(4), 3931 (2017)
11. R. Valentino, W.-S. Jung, Y.-B. Ko, Opportunistic computational offloading system for clusters of drones, in *2018 20th International Conference on Advanced Communication Technology (ICACT)* (IEEE, 2018), pp. 303–306
12. C. Hou, G. Liu, Q. Tian, Z. Zhou, L. Hua, Y. Lin, Multi-signal modulation classification using sliding window detection and complex convolutional network in frequency domain. IEEE Internet Things J. (2022). https://doi.org/10.1109/JIOT.2022.3167107
13. Y. Lin, Y. Tu, Z. Dou, An improved neural network pruning technology for automatic modulation classification in edge devices. IEEE Trans. Veh. Technol. **69**(5), 5703–5706 (2020)
14. K. Eritmen, M. Keskinoz, Improving the performance of wireless sensor networks through optimized complex field network coding. IEEE Sens. J. **15**(5), 2934–2946 (2014)
15. K. Eritmen, M. Keskinoz, Symbol-error rate optimized complex field network coding for wireless communications. Wireless Netw. **21**(8), 2467–2481 (2015)
16. H. Phan, F.-C. Zheng, M. Fitch, Wireless backhaul networks with precoding complex field network coding. IEEE Commun. Lett. **19**(3), 447–450 (2015)
17. Y. Dong, X. Jiang, H. Zhou, Y. Lin, Q. Shi, Sr2cnn: zero-shot learning for signal recognition. IEEE Trans. Signal Process. **69**, 2316–2329 (2021)
18. Y. Lin, Y. Tu, Z. Dou, L. Chen, S. Mao, Contour stella image and deep learning for signal recognition in the physical layer. IEEE Trans. Cogn. Commun. Netw. **7**(1), 34–46 (2020)
19. Y.-F. Wang, J.-H. Lee, A zf-based precoding scheme with phase noise suppression for massive mimo downlink systems. IEEE Trans. Veh. Technol. **67**(2), 1158–1173 (2017)
20. Z. Liu, G.B. Giannakis, S. Zhou, B. Muquet, Space-time coding for broadband wireless communications. Wirel. Commun. Mob. Comput. **1**(1), 35–53 (2001)
21. R. Xue, M. Zhao, H. Tang, Information transmission schemes based on adaptive coded modulation for UAV surveillance systems with satellite relays. IEEE Access **8**, 191355–191364 (2020)
22. Y. Wen, L. Wu, A modified sphere detection algorithm with lower complexity for mimo detection, in *2017 International Conference on Communication, Control, Computing and Electronics Engineering (ICCCCEE)* (IEEE, 2017), pp. 1–4
23. J. Li, W. Li, A novel sphere detection algorithm for mqam mimo systems, in *2016 IEEE International Conference on Electronic Information and Communication Technology (ICEICT)* (IEEE, 2016), pp. 34–37

Publisher's Note